Effect of Plasma Liquid on Colloidal (CoNPs) and (PtNPs) Nanostructures Produced by Laser Ablation Technique for Antibacterial Applications

Entidhar Jasim Khamees
University of Babylon
Halah Mohammed Azeez
University of Babylon
Ahmed Shaker Hussein
University of Babylon
Rafea T. Ahmed
University of Babylon
Olcay Gençyılmaz (ogencyilmaz@karatekin.edu.tr)
Çankırı Karatekin University

Research Article

Keywords: Colloidal nanoparticles platinum (PtNPs), cobalt (CoNPs), Laser Ablation (PLAL), Antibacterial activity

Posted Date: January 18th, 2023

DOI: https://doi.org/10.21203/rs.3.rs-2487441/v1

Abstract

In this work, the biological and physical properties of colloidal platinum (PtNPs) and cobalt (CoNPs) nanoparticles were examined for antibacterial applications. The colladial PtNPs and CoNPs nanoparticles were produced using two different liquids (double-distilled water (DDDW) and Dulbecco's Modified Eagle's Medium (DMEM)) by laser ablation technique (PLAL). Characterization techniques such as transmission electron microscopy (TEM), UV-vis spectroscopy and Fourier transform infrared (FTIR) were used to determine some physical properties of PtNPs and CoNPs. The antibacterial effects ofcolladial PtNPs and CoNPs at different doses on various bacteria were investigated and their antibacterial activity resistances were calculated by measuring the inhibition zone widths. The effect of the liquid used in the production, the type of bacteria and dose amounts on the antibacterial resistance of these nanoparticles were determined. In this study, it has been shown that the liquid used in the production of PtNPs and CoNPs can create significant changes in the physical and antibacterial properties of nanoparticles, especially by changing the size and concentration of collodial PtNPs.

1. Introduction

Nanotechnology has a significant influence on a variety of scientific and technological sectors, including health, electronics, energy, and the space industry. Nanoparticles have distinct physicochemical, optoelectronic and biomedical properties that can be useful in various applications [1].

Colloidal nanoparticles can show different physcachemical, optical, magnetic, catalytic, antibacterial and pharmaceutical agents properties depending on the production techniques. Therefore, many studies have been carried out recently on the production, characterization and application areas of colladial particles [2]. Colloidal platinum (Pt) and cobalt (Co) nanoparticles are frequently used in materials science, physics and chemistry [3]. Platinum (Pt) is an important nanoparticle that may have biological applications such as DNA damage glycation, cancer therapy, glucose sensors [4] and cancer therapy [5, 6]. Platinum nanoparticles (PtNPs) are important in a variety of sectors, including medicine [7]. Pectin and sodium borohydride were used as capping and reducing agents for the synthesis of platinum nanoparticles with strong antibacterial activity [8]. The two primary approaches to NP synthesis are the bottom-up method and the top-down approach. A top-down technique is demonstrated by the ablative pulsed laser (APL) [9]. The ablation of solids in liquid environments, such as metals, semiconductors, ceramics, and alloys, is a practical method for the synthesis of nanomaterials (pure water or a water solution of a stabilizing agent). This method creates very pure nanoparticles with less agglomeration and is noticeably simpler to utilize than chemical methods. Using APL in liquid, PtNPs of various sizes, shapes, and properties may be created. [10]. The production of high-purity PtNPs in pure water has proven successful [11–14]. Cobalt oxide (Co_3O_4) is a transition metal oxide and a p-type semiconducting material [12]. They have also been employed as photocatalysts in antibacterial, antioxidant, and anticancer applications, as well as for the breakdown or adsorption of dyes and organic pollutants. CoNPs have promising remediation potential since they are effective at degrading contaminants for which they have an affinity and are also less costly than noble metals [15, 16]. Because of their high surface area, CoNPs have gained a lot of

attention because they are less expensive than noble metal nanoparticles (NPs) and have various characteristics, such as electrical and magnetic. CoNPs have been investigated as a therapeutic agent for disorders such as microbial infection, making them appealing for biomedical uses. CoNPs are harmless in the body at low concentrations, exhibit high antibacterial and antifungal activity at low doses, and have fewer adverse effects than antibiotics [7, 17, 18]. The capacity to create multifunctional nanoparticles that can perform a variety of biological tasks is seen as a significant achievement. Nanotechnology encompasses materials, thin films, and electronics manufactured at this size. The diameter range should only be expanded from 1 to 100 nm [18]. Functional nanoparticles have been covalently bonded to biological components such as peptides, proteins, nucleic acids, or small-molecule ligands to carry out certain tasks [21–23].

Different production techniques of nanoparticles have been reported as sol-gel, chemical reduction, thermal decomposition, microwave irradiation, radiolysis, ultrasonic irradiation, and laser ablation [15]. Among these techniques, laser ablation involves irradiating a solid with a laser beam to remove the materials from it.; [6, 7]. Pulsed laser ablation (PLAL) in liquid is an economical and practical technique that does not require vacuum and the main use is weak agglomeration and impurity-free.

In this study, we produced colloidal PtNPs and CoNPs nanoparticles using pulsed laser ablation (PLAL) technique in different liquid medium and were reported the effect of liquid medium on the structural, optical and molecular properties. In addition, the antibacterial activity of colloidal PtNPs and CoNPs was investigated. These nanoparticles were researched in the fight against antibiotic-resistant bacteria and their effectiveness against antibiotic-resistant microbes was determined.

2. Experimental Details

2.1. Production of PtNPs and CoNPs

In this study, the production of PtNPs and CoNPs nanoparticles was produced using laser ablation technique. Colloidal solutions of PtNPs and CoNPs nanoparticles were prepared in double-distilled water (DDDW) and Dulbecco's Modified Eagle's Medium (DMEM) using the pulsed laser ablation technique, by bombarding a high-purity (99.99%) (platinum and cobalt) target. Experimental details are given Table 1 and Fig. 1.

Table 1
Experimental parameters

Nanoparticles	PtNPs and CoNPs	PtNPs and CoNPs
Liquids	Double-distilled water	DMEM
Laser type	Nd-YAG laser	Nd-YAG laser
Wavelength	1064 nm	1064 nm
Average power	600 mJ	600 mJ
Pulse	300	300
Intensity	12.23 J/m^3	12.23 J/m^3
Pulse duration	10 nanoseconds	10 nanoseconds
Repetition frequency	6 Hz	6 Hz
Temperature	37 °C	37 °C
Focus Diameter	3.5	3.5

Figure 1

2.2. Characterization of PtNPs and CoNPs

The structural, optical and molecular properties of PtNPs and CoNPs were investigated using Transmission Electron Microscope (TEM), Fourier-transform infrared spectroscopy (FTIR), UV-Visible spectphotometer (UV-vis). TEM analysis was carried out using a Hitachi H-7650, Germany model Transmission Electron Microscope and the size distribution and shape of NPs was obtained by these measurement. For optical anayysis, UV-Visible absorption spectra measurements were carried out using a UVIR-210A SHIMADZU spectrophotometer over a wide range of wavelengths (200–900 nm). The FTIR spectrum is recorded using a range of (500–4000) cm^{-1} for the suspension to validate the creation of PtNPs and CoNPs.

The bacteria strains used to determine the antibacterial activity were escherichia coli (E. coli) and bacillus subtilis (B. subtilis). These strains were calculated using the Kirby Bauer disc diffusion method. The antibacterial activity tests were examined for PtNPs and CoNPs prepared in both DDDW and DMEM for E. coli and B. subtilis bacteria. These samples were named separately and are given in Table 2.

Table 2
The name of PtNPs and CoNPs for antibacterial activity test

Nanoparticles	Liquids	
	Double-distilled water (DDDW)	Dulbecco's Modified Eagle's Medium (DMEM)
CoNPs	CoNPs0	CoNPs1
PtNPs	PtNPs2	PtNPs3

2.3. Statistic evaluation

All information was reported as mean SD in the results section. One-way analysis of variance was used to evaluate the data using the software sigma plot v12 (ANOVA).

3. Results And Discussion

3.1. TEM anaylsis of PtNPs and CoNPs

Figure 2 (a) and (b) shows the TEM images and particle size distribution corresponding to TEM analysis of PtNPs obtained under different ablation liquids, respectively. Figure 1 shows that PtNPs have a spherical shape, with little aggregation observe in the as-prepared DDDW and DMEM liquids. It was determined that the grain sizes of PtNPs3 produced in DMEM have smaller than PtNPs2 produced in water. PtNPs2 produced in DDDW have a more heterogeneous structure compared to the others. Because of this, the particles clustered together and the PtNPs2 are more opaque. This case also affected the absorption of the PtNPs2 nanoparticles (Fig. 4 (a)).

Figure 2 (b) shows PtNPs2 and PtNPs3 nanoparticles the particle size distribution histogram. The particle sizes of PtNPs2 nanoparticles ranged from 5 to 40 nm while the particle sizes of PtNPs3 nanoparticles were about 5 to 50 nm.

Spherical PtNPs2 and PtNPs3 nanoparticles of average particle size varies are obtained as 12–20 nm, respectively. The particle size of PtNPs produced in water was obtained smaller than the others.

Figure 2

Figure 3 (a) and (b) shows the TEM images and particle size distribution corresponding to TEM analysis of CoNPs obtained under different ablation liquids, respectively. The CoNPs showed a rod and spherical shape with few aggregations that were observed in the medium of double distilled water and DMEM nanoparticles (Fig. 3). The particle sizes ranged from 15 to 55 nm, with an average of 38 nm.

Figure 3

3.2 Optical absorption analysis

Figure 4 shows absorbance spectra of PtNPs and CoNPs nanoparticles. According to Fig. 4 (a), the absorption edge of PtNPs2 nanoparticles produced in water was observed at long wavelengths while that of PtNPs3 nanoparticles produced in DMEM was observed at shorter wavelengths. In addition, the band edge structure nad absorsbans values changed depending on the type of liquid used. PtNPs2 nanoparticles have higher absorbance value than PtNPs3 while PtNPs3 nanoparticles have shaper band edge than PtNPs2. This depends on the particle size and distribution of the nanoparticles. TEM analysis also support this results. When Fig. 4 (b) is examined, it is seen that there is much variation between the absorption spectra of CoNPs nanoparticles.

Figure 4

The band values of CoNPs and PtNPs were calculated by the following relation [32]:

$(\alpha h\nu) = A(h\nu - E_g)^{n}$ (1)

where *A* is a constant that depends on refractive index of the material, E_g is the optical band gap, *hv* is the photon energy. Figures (5) shows the value of (Eg) obtained for the direct energy transition from plotting between the linear part of $(\alpha h\nu)^2$ versus ($h\nu$). Likewise from the Figure (5), one can extract the band gap as 2.3 and 2.7 eV for the PtNPs2,and PtNPs3 nanoparticles the band gap as 4.4 and 4 eV for the CoNPs0 and CoNPs1.

Table 3
The radius of CoNPs and PtNPs nanoparticles

Nanoparticles	Absorbance peak point	Particle r (nm)
CoNPs0	355	1.342
CoNPs1	350	2.406
PtNPs2	471	1.050
PtNPs3	466	653.9

In addition, the average particle size was calculated using the absorption spectra of NPs. First of all, inflection points in the absorption spectra were determined. In the particle size calculations, it was determined using the effective mass model, which describes the particle size (r, radius) of the nanoparticles as a function of the peak absorption wavelength (λ_p) [33] .

$$\mathrm{r\,(nm)} = \frac{\left[\frac{1020{,}72}{\mathrm{p}}\right]^{1/2} - (0{,}3049)}{\frac{2483{,}2}{\mathrm{p}} - 6{,}3829}$$

2

During the derivation of Eq. (2), m_e = 0.26 m_o, m_h = 0.59m_o, m_o is the free electron mass, ε = 8.5, and bulk E_g = 3.3 eV [34]. Particle sizes of CoNPs and PtNPs are given in Table 3 The lowest particle size was PtNPs3, while the highest particle size was formed in CoNPs1 material. The size values of CoNPs0 and PtNPs2 particles are close to each other. It was found that the particle size of both CoNPs and PtNPs materials decreased in the DMEM liquid. It was determined that water did not have a significant effect on the sizes of CoNPs and PtNPs nanoparticles.

Optical transitions between the valence and conduction band in a material, defect states, conduction mechanisms and defects caused by disproportionate charge depend on the material's bandwidth. Detection of these changes and defects in the structure is made by detecting the Urbach tails formed in the band structure. The energy associated with these imperfect Urbach tails in the band structure is defined as the Urbach energy. Therefore, it is an important parameter for the detection of changes in the band structure of the materials. The Urbach energy were calculated by taking inverse of the slope of equetion [35].

$$\alpha = \alpha_0 exp^{h-E/E_u}$$

3

where E and α_0 are a constant and E_u is the Urbach energy interpreted as the width of the tails of localized states, in the band gap. Figure 6 shows *lnα-hv* graphs.

Figure 6

Another important parameter showing the change in the band structure is the stepness parameter. This parameter is a perpendicularity parameter that indicates the band broadening in the material. Futhermore, the stepness parameter determines the electron-phonon interaction. These two important parameters can be calculated with the following equations [34, 35].

$$= \frac{k_B T}{E_u}$$

4

$$E_{e-p} = \frac{2}{3}$$

5

where σ is steepness parameter, k_B is Boltzmann constant, T is absolute temperature and $E_{e\text{-}p}$ is electron-phonon interaction. Also, we calculated the refractive index of CoNPs and PtNPs using Ravindra relation [36] .This relation related to tne band gap of material. This equation is given below:

$$n = 4{,}084 - 0{,}62E_g$$

6

where E_g is optical band gap energy calculated from Tauc plot and n is refractive index.

In additon to, Fig. 7 and Fig. 8 shows varitions of optical band gap-Urbach energy and stepness parameter-electron phonon interaction, respectively. The porosity values of CoNPs and PtNPs were calculated using Eq. (6), a quantitative analysis on porosity based on refractive index [37].

$$Porosity\,(\%) = \left[1 - \frac{n^2 - 1}{n_d^2 - 1}\right] \times 100$$

7

where, n is the refractive index of the CoNPs and PtNPs and n_d is the refractive index values of the pore-free CoNPs and PtNPs known in the literature. These calculated refractive index and prosity values has also been given in Table 4. In this study, while the refractive index values of PtNPs were consistent with the literature in both DDDW and DMEM fluids, the refractive index values of CoNPs were low in both water and DMEM fluids. It was determined that PtNPs produced in water had the lowest porosity value and CoNPs had the highest value. Also, the porosity values are lower when produced in DDDW while it is lower in DMEM fluid for CoNPs.

Table 4
The some optical parametres of CoNPs and PtNPs obtained under different ablation liquids

Nanoparticles	E_g (eV)	E_u (eV)	Stepness Parameter (σ)	Refractive index (n)	Porosity (%)	Ee-p
CoNPs0	4.0	4.70	$8.02{\cdot}10^{22}$	1.60	62.9	$5.34{\cdot}10^{-22}$
CoNPs1	4.4	1.76	$2.14{\cdot}10^{21}$	1.32	55.0	$1.42{\cdot}10^{-22}$
PtNPs2	2.7	0.20	$1.88{\cdot}10^{20}$	2.41	32.6	$3.54{\cdot}10^{-21}$
PtNPs3	2.3	0.44	$8.56{\cdot}10^{21}$	2.65	37.4	$7.78.^{10-23}$

Figure 7

Figure 8

3.3. FTIR Analysis

The PtNPs and CoNPs nanoparticles were analyzed using FTIR to determine the biomolecules involved in nanoparticle stabilization in solution. Figure 9 shows transmittance spectra of PtNPs and CoNPs nanoparticles obtained under different ablation liquids. In Fig. 9, PtNPs-S2 generated by laser ablation with DDDW and DMEM, the spectrum PtNP-S3 was recreded in range (500–5000 cm ¹) this shows the peaks at [3319.46 cm ¹, 1637.14cm ¹ and 598.45cm ¹] The peak at 1637.14 cm ¹ belongs to the C-H bending aromatic compound, whereas the peak at 3319.46 cm ¹ relates to the O-H stretching bond. The C-I vibration was linked to the band at about 598.45cm ¹. The spectrum PtNPs2 was recrded in range [3324.98 cm ¹,1636.54 cm ¹ and 577.60 cm ¹] correspond to an whereas the peak at 3324.98 cm ¹ medium, N-H stretching bond and 636.54 cm ¹ belongs to the C = C stretching band. and 577.60 cm ¹ C = C strong band.

The IR spectra of the manufactured CoNPs revealed that laser ablation with double-distilled water and DMEM produced a sequence of absorption peaks ranging from 500 to 5000 cm1 (Fig. 4 red and black) CoNPs-S0 this shows the peaks at [3330.76, 2973.38, 1379.74, 1087.21, 1045.07 ,879.67, 634.84]cm ¹ and CoNPs-S1 this shows the peaks at [3319.23 ,2973.37, 1380.10, 1087.12, 1045.09, 879.74, 635.09]cm ¹. The powerful and broad peak located at 3330.76 cm ¹,3319.23 cm ¹ assigned to N-H stretching bond. and the peak at 2973.38 cm ¹, 2973.37 cm ¹ corresponds to the C-H stretching bending mode bond, and broad peak lacated at 1380.10 cm ¹, 1379.74 cm ¹ assigned to S = O stretching bond, the peak at 1087.2,11087.12 cm ¹ and 1087.12, 1045.09 cm ¹ corresponds to the C-O stretching bond, the peak at 879.67 and 879.74 cm ¹ corresponds to the C = C bending mode bond, and the peak at [634.84, 635.09]cm ¹ assigned to C-I stretching halo compound.

Figure 9

3.4. Antibacterial activity of PtNPs and CoNPs

Figure 10 (a) and (b) show antibacterial effect of PtNPs and CoNPs nanoparticles obtained under different ablation liquids (double-distilied water and DMEM) on two different types of bacteria. Figure 10 (c) and (d) the zone of inhibition measurements against E. coli and B. subtilis. These CoNPs showed no toxicity against E. coli and B.subtilis but it showed significant toxicity toward PtNPs-S2 represent generated by laser ablation with double-distilled water and PtNPs-S3 generated by laser ablation with DMEM toxicity against E. coli and B.subtilis show more toxicity. Zone of inhibition measurements against E. coli and B. subtilis are shown graphically as shown Fig. 10 (c) and (d).

Figure 10

High purity platinum nanoparticles (PtNPs) with two particle sizes (platinum nanoparticles generated in double-distilled water and DMEM). The particle size was seen to range from 5 to 40 nm, with an average

size of 12 nm, whereas the particles generated in DMEM medium ranged from 5 to 50 nm, with an average particle size of 20 nm.) The laser ablation approach was used to effectively synthesize it. PtNPs' antimicrobial action has long been of particular interest. Using the laser ablation process, it was effectively synthesized. The Pt nanoparticles were spherical in form, and their diameters shrank as the number of pulses increased. These qualities are controllable and are determined by laser parameters such as pulse rate, pulse energy, irradiation period, target material type, and the nature of the liquid in which the material is submerged [16, 7, 17]. PtNPs have been studied for their antibacterial properties. Akther and his colleagues show that PtNPs reduce biofilm development. They discovered that attaching these particles to bacterial surfaces can cause cell wall rupture or membrane lysis. These effects are connected to the production of intracellular ROS, which results in the production of cytokines associated with ROS [26–28]. This study evaluated the antibacterial resistance of Co NPs against two widespread pathogens, including E. coli and B. subtilis. The in vitro examination results showed that the Co NPs had weak antibacterial activity, suggesting that they might not be able to eradicate germs that are resistant to many drugs or be used to cure disease [14]. The theory put out by the authors was that once the nanoparticles accumulated past a certain point, they would eventually lose their capacity to enter the bacteria cell. According to a report, the surface-to-volume ratio rises as nanoparticle size decreases, suggesting that the nanoparticles' size may have a significant impact on the antibacterial activity [7, 30]. Cobalt nanoparticles (CoNPs) were created by laser ablation and were proven to be so by TEM and FTIR studies (s0 represent generated with double-distilled water and s1 generated by DMEM with a size ranging from (20nm to 70 nm). Nanorods with a rounded form and smooth surface were visible in the nanoparticles. This study evaluated the antibacterial resistance of CoNPs against Escherichia coli and B. subtilis, two common microorganisms. The outcomes of the in vitro test showed that the CoNPs had marginal antibacterial activity.Further studies are required to explore the antibacterial effect beyond this in the size of the nanoparticles.

4. Conclusions

The linking of PtNPs with biological liquid is an essential step in the therapeutic chain to achieve the endocytosis of PtNPs by bacterial. This phase is completed within the stages of preparation of the NPs synthesis liquids within the chemical or biological methods, but in this study, the binding process was accomplished by making DMEM a synthesis medium of the produced PtNPs by PLAL. The size and concentration of PtNPs are affected by the laser parameters and the surrounding medium as the physical measurements have been demonstrated.

The biological tests have shown that ptNPs have ability to couple with the bacteria by depending on their size and concentration.

The plasmonic absorption for the incubated cells with the absorption peaks of PtNPs confirms the accumulation by linear form, which has been a favorite to be used in the IR region and has given satisfying results in the killing percentages of both E. coli and B. subtilis.

As for the cobalt nanoparticles, they showed little effect on E. coli and B. subtilis. For both mediums, they need more study through the use of more laser energies, as well as less size and different concentrations. Particle sizes of CoNPs and PtNPs produced in DMEM fluid were reduced.

Declarations

ACKNOWLEDGEMENT

I like to thank both departments very much. Both the Biology Department at the College of Science and the Laser Department at the College of Girls' Sciences at the University of Babylon.

CONFLICT OF INTEREST

Regarding the publishing of this work, the authors affirms that there are no competing interests.

References

1. Jeyaraj, M., Gurunathan, S., Qasim, M., Kang, M.H., Kim, J.H.: A comprehensive review on the synthesis, characterization, and biomedical application of platinum nanoparticles. Nanomaterials. **9**, 1–41 (2019)
2. Jan, H., Gul, R., Andleeb, A., Ullah, S., Shah, M., Khanum, M., Ullah, I., Hano, C.: Haider Abbasi, A detailed review on biosynthesis of platinum nanoparticles (PtNPs), their potential antimicrobial and biomedical applications. J. Saudi Chem. Soc. **25**(8), 101297 (2021)
3. Yu, H., Braun, P., Yildirim, M.A., Lemmens, I.: High-quality binary protein interaction map of the yeast interactome network. Science. **322**, 104–110 (2008)
4. Zhai, D., Liu, B., Shi, Y., Pan, L., Wang, Y., Li, W., Zhang, R., Yu, G.: Highly sensitive glucose sensor based on pt nanoparticle/polyaniline hydrogel heterostructures. ACS Nano. **7**(4), 3540–3546 (2013)
5. Dasari, S., Tchounwou, P.B.: Cisplatin in cancer therapy: molecular mechanisms of action. Eur. J. Pharmacol. **740**, 364–378 (2014)
6. Tunçer, S., Çolakoğlu, M., Ulusa, S., Ertas, G., Karasu, Ã., Banerjee, S.: Evaluation of colloidal platinum on cytotoxicity, oxidative stress and barrier permeability across the gut epithelium. Heliyonm. **5**, e01336 (2019)
7. Jyothi, L., Kuladeep, R., Rao, D.N.: Solvent effect on the synthesis of cobalt nanoparticles by pulsed laser ablation: their linear and nonlinear optical properties. J. Nanophotonics. **9**(1), 093088 (2015)
8. Russo, R.E., Mao, X., Gonzalez, J.J., Zorba, V., Yoo, J.: Laser ablation in analytical chemistry. Anal. Chem. **85**(13), 6162–6177 (2013)
9. Ayaz Ahmed, K.B., Raman, T., Anbazhagan, V.: Platinum nanoparticles inhibit bacteria proliferation and rescue zebrafish from bacterial infection. RSC Adv. **6**, 44415–44424 (2016)
10. Prepared, P.C.V.: Impact of Platinum Nanoparticles and Laser Lights Combination on Hep-G_2 Cancer Cell Line. J. Xidian Univ. **14**(9), 0–1 (2020)

11. Lazar, O.A., Moise, C.C., Nikolov, A.S., Enache, L.B., Mihai, G.V., Enachescu, M.: The Water-Based Synthesis of Platinum Nanoparticles Using KrF Excimer Laser Ablation. Nanomaterials. **12**(3), 1–18 (2022)
12. Madlum, K.N., Khamees, E.J., Abdulridha, S.A., Naji, R.A.: Antimicrobial and Cytotoxic Activity of Platinum Nanoparticles Synthesized by Laser Ablation Technique. J Nanostruct. **11**(1), 13–19 (2021)
13. Loza, K., Heggen, M., Epple, M.: Synthesis, Structure, Properties, and Applications of Bimetallic Nanoparticles of Noble Metals. Adv. Funct. Mater. **30**(21), 1–14 (2020)
14. Azrahuddin, M., Zhu, G.H., Das, D., Özgür, E., Uzun, L., Turner, A.P.F., Patra, H.K.: A repertoire of biomedical applications of noble metal nanoparticles. Chem. Commun. **55**, 6964–6996 (2019)
15. Anele, A., Obare, S., Wei, J.: Recent Trends and Advances of Co_3O_4 Nanoparticles in Environmental Remediation of Bacteria in Wastewater, Nanomaterials, 12 (7) 2022
16. Khusnuriyalova, A.F., Caporali, M., Hey-Hawkins, E., Sinyashin, O.G., Yakhvarov, D.G.: Preparation of Cobalt Nanoparticles. Eur. J. Inorg. Chem. **30**, 3023–3047 (2021)
17. Waris, A., Din, M., Ali, A., Afridi, S., Baset, A., Khan, A.U., Ali, M.: Green fabrication of Co and Co_3O_4 nanoparticles and their biomedical applications: A review. Open. Life Sci. **16**(1), 14–30 (2021)
18. Pereira, M.S., Vasconcelos, M.S., Palacio, V.M.R., da Silva Oliveira, M.P., de Santos, F.G.S., Mourão, L.P. dos, Vasconcelos, D.L.M., Freire, P.T., C.Vasconcelos, I., Frota: Characterization of $CoFe_2O_4$, $NiFe_2O_4$, and $ZnFe_2O_4$ Nanoparticles Synthesized by a Proteic Sol-gel Method, J. Supercond. Nov. Magn. 34 (11) 2845–2853. (2021)
19. Tawfeeq, A.T.: Pulsed laser ablation synthesized silver nanoparticles induce apoptosis in human glioblastoma cell line and possess minimal defect in mice brains. Iraqi J. Biotechnol. **12**(2), 92–106 (2013)
20. Beyth, N., Houri-Haddad, Y., Domb, A., Khan, W., Hazan, R.: Alternative antimicrobial approach: Nano-antimicrobial materials, Evidence-based Complement. Altern. Med. 2015:246012. (2015)
21. Abed, A., Derakhshan, M., Shirazinia, M.K.M., Mahjoubin-Tehran, M., Homayonfal, M., Hamblin, M.R., Mirzaei, S.A., Soleimanpour, H., Dehghani, S., Dehkordi, F.F.: Platinum Nanoparticles in Biomedicine: Preparation, AntiCancer Activity, and Drug Delivery Vehicles. Front. Pharmacol. **13**, 1–23 (2022)
22. Verma, S., Utreja, P., Rahman, M., Kumar, L.: Gold Nanoparticles and their Applications in Cancer Treatment. Curr Nanomed. **8**(3), 184–201 (2018)
23. Kanwal, Z., Raza, M.A., Riaz, S., Manzoor, S., Tayyeb, A., Sajid, I., Naseem, S.: Synthesis and characterization of silver nanoparticledecorated cobalt nanocomposites (Co@AgNPs) and their density-dependent antibacterial activity. R Soc. Open. Sci. **6**(5), 1–15 (2019)
24. Khamees, E.J.: Physical and biological synthesis of GNPs and keratin nanoparticles from chicken's feather and applications, IOP Conference Series: Materials Science and Engineering 928 (7) (2020)
25. Mendivil Palma, M.I., Krishnan, B., Rodriguez, G.A.C., Das Roy, T.K., Avellaneda, D.A., Shaji, S.: Synthesis and Properties of Platinum Nanoparticles by Pulsed Laser Ablation in Liquid. J. Nanomater. **9651637**, 1–12 (2016)

26. Akther, T., Khan, M.S., Srinivasan, H.: Novel silver nanoparticles synthesized from anthers of couroupita guianensis Abul. Control growth and biofilm formation in human pathogenic bacteria. Nano Biomed. Eng. **10**(3), 250–257 (2018)
27. Khumaeni, A., Alhamid, M.Z., Anam, C., Budiono, A.: Synthesis of Colloidal Silver, Platinum, and Mixture of Silver-Platinum Nanoparticles Using Pulsed Laser Ablation as a Contrast Agent in Computed Tomography. Iran. J Med Phys. **19**(1), 49–57 (2022)
28. Gopal, J., Hasan, N., Manikandan, M., Wu, H.F.: Bacterial toxicity/compatibility of platinum nanospheres, nanocuboids and nanoflowers. Sci. Rep. **3**, 1–8 (2013)
29. Sulaiman, J.M.A., Hamdoon, S.M., Abdulrahman, G.Y.: Antibacterial activity of cobalt ferrite (CoFe2O4) nanoparticles against oral enterococci. Mater. Sci. Forum. **1021**, 150–159 (2021)
30. Gupta, V., Kant, V., Sharma, A.K., Sharma, M.: Comparative assessment of antibacterial efficacy for cobalt nanoparticles, bulk cobalt and standard antibiotics: A concentration dependant s. Nanosyst Phys. Chem Math. **11**(1), 78–85 (2020)
31. Jafarirad, S., Mehrabi, M., Divband, B., Kosari-Nasab, M.: Biofabrication of zinc oxide nanoparticles using fruit extract of Rosa canina and their toxic potential against bacteria: a mechanistic approach. Mater. Sci. Engineering: C. **59**, 296–302 (2016)
32. Pesika, N.S., Stebe, K.J., Searson, P.C.: Relationship between absorbance spectra and particle size distributions for quantum-sized nanocrystals. J. Phys. Chem. B. **107**(38), 10412–10415 (2003)
33. Soosen, S.M., Bose, L.: George, Optical properties of ZnO nanoparticles. Acad. Rev. **16**, 57–65 (2009)
34. Urbach, F.: The long-wavelength edge of photographic sensitivity and of the electronic absorption of solids. Phys. Rev. **92**(5), 1324 (1953)
35. Singh, J., Verma, V., Kumar, R., Kumar, R.: Influence of Mg^{2+} substitution on the optical band gap energy of $Cr_{2-x}Mg_xO_3$ nanoparticles. Results in Physics. **13**, 102106 (2019)
36. Vettumperumal, R., Kalyanaraman, S., Santoshkumar, B., Thangavel, R.: Estimation of electron–phonon coupling and Urbach energy in group-I elements doped ZnO nanoparticles and thin films by sol–gel method. Mater. Res. Bull. **77**, 101–110 (2016)
37. Bhardwaj, N., Gaur, A., Yadav, K.: Effect of doping on optical properties in $BiMn_{1-x}(TE)_xO_3$ (where x = 0.0, 0.1 and TE = Cr, Fe, Co, Zn) nanoparticles synthesized by microwave and sol-gel methods. Appl. Phys. A. **123**(6), 1–7 (2017)
38. Yoldas, B.E., Partlow, D.P.: Formation of broad band antireflective coatings on fused silica for high power laser applications. Thin solid films. **129**(1–2), 1–14 (1985)

Figures

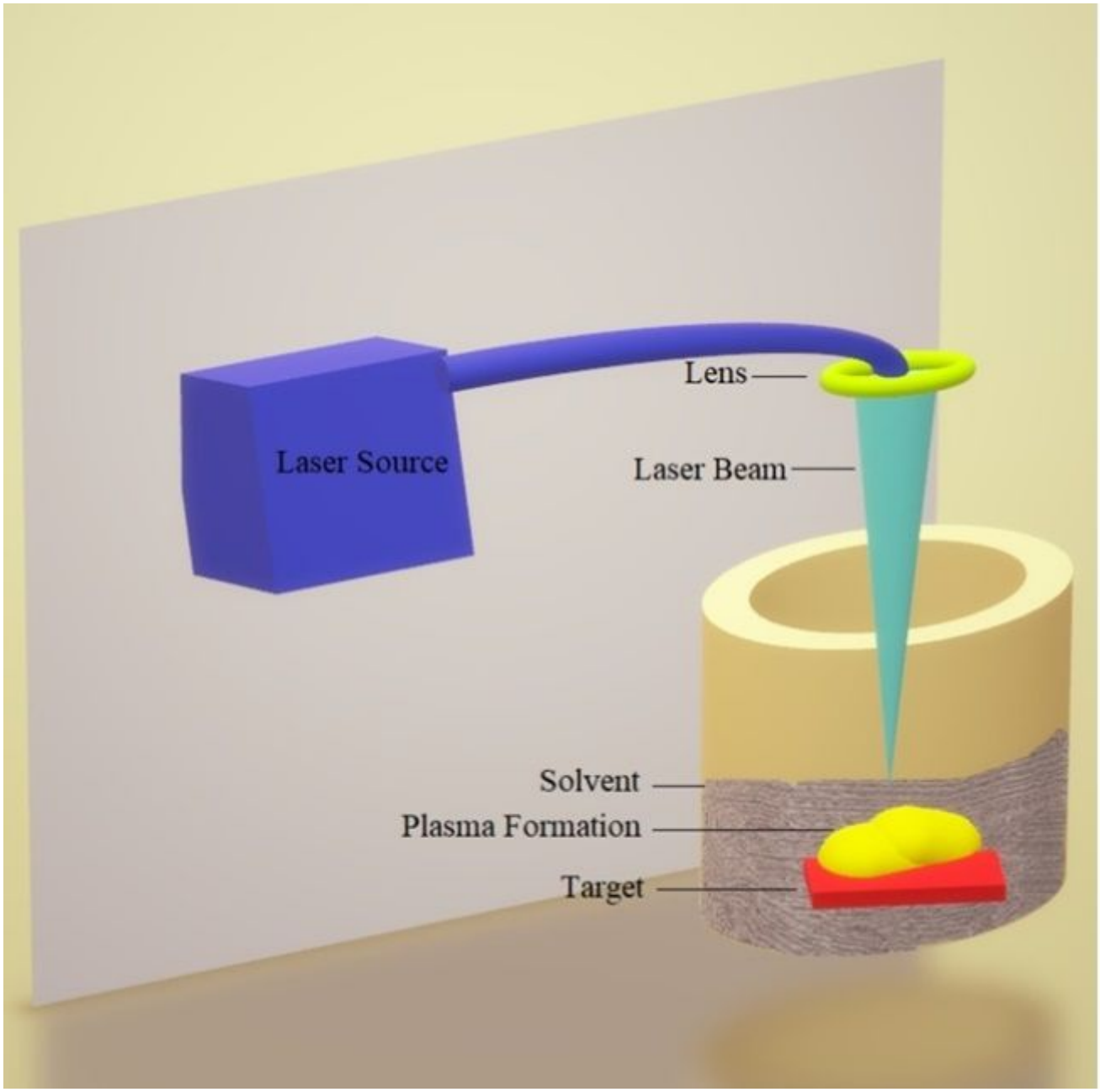

Figure 1

The pulsed laser ablation (PLAL) technique presentation

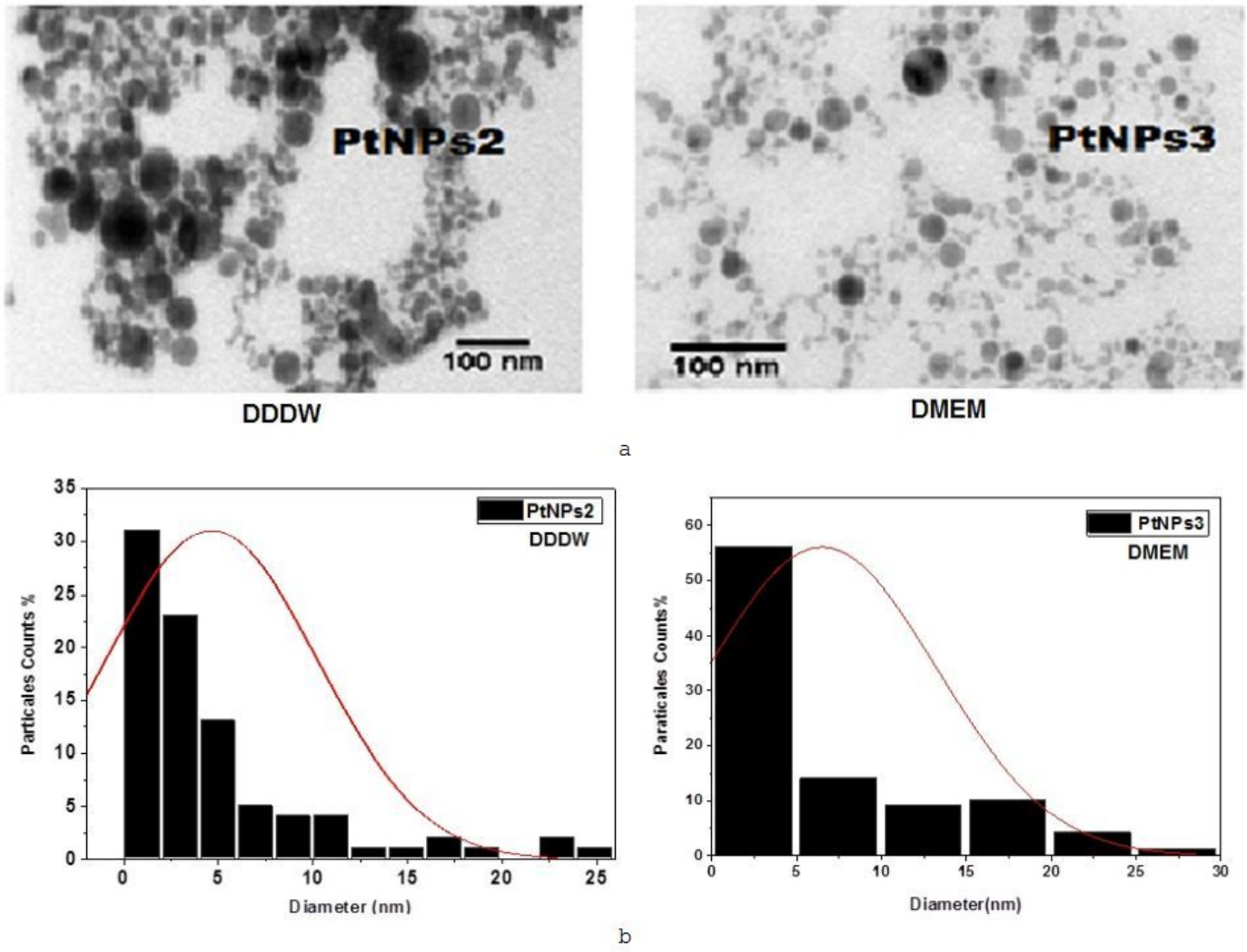

Figure 2

TEM results of PtNPs obtained under different ablation liquids a) TEM images and b) The particle size distribution

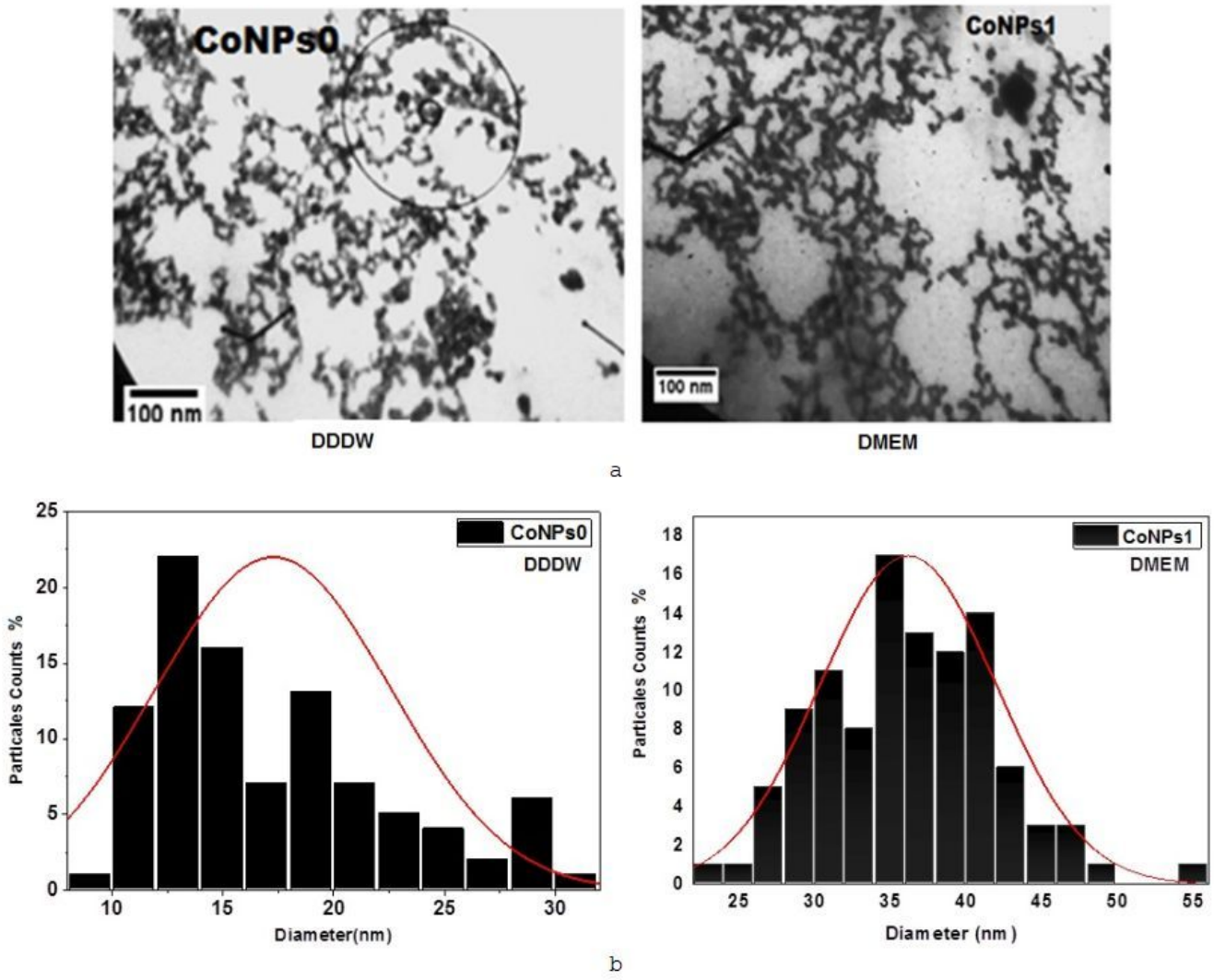

Figure 3

TEM results of CoNPs obtained under different ablation liquids a) TEM images and b) The particle size distribution

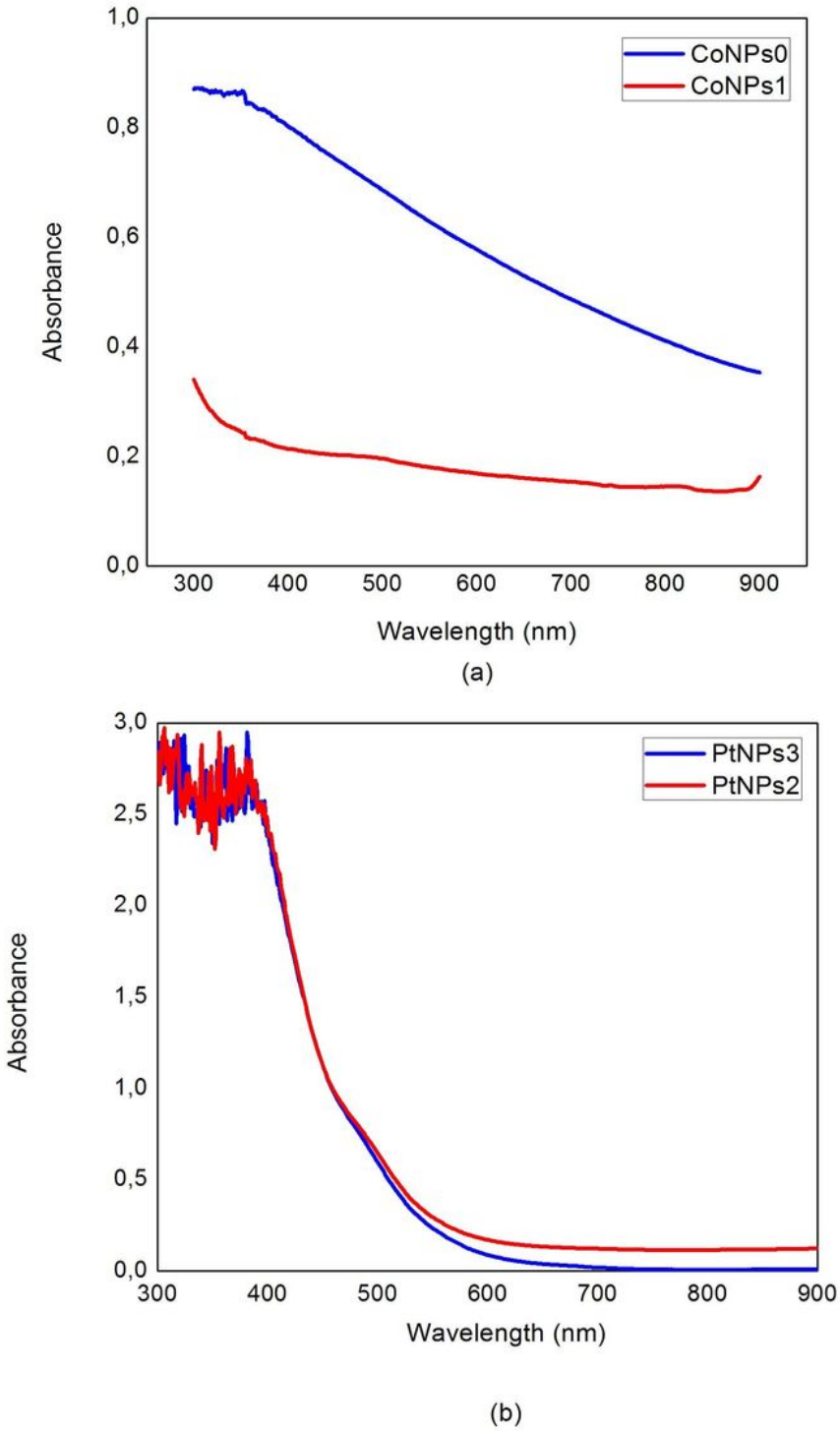

Figure 4

UV-Vis absorbance spectrum of CoNPs and PtNPs obtained under different ablation liquids a) CoNPs and b) PtNPs

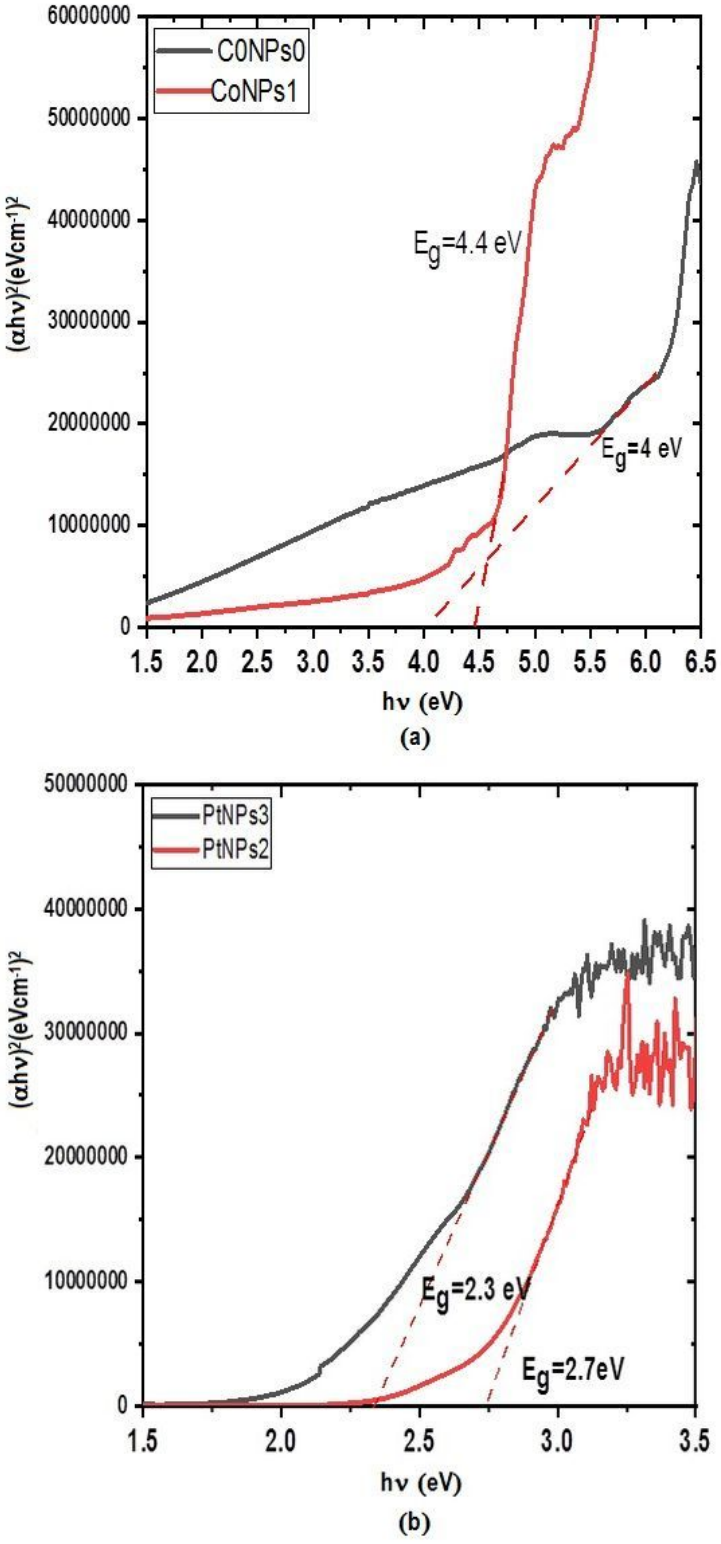

Figure 5

The optical energy gaps of CoNPs and PtNPs obtained under different ablation liquids a) CoNPs and b) PtNPs

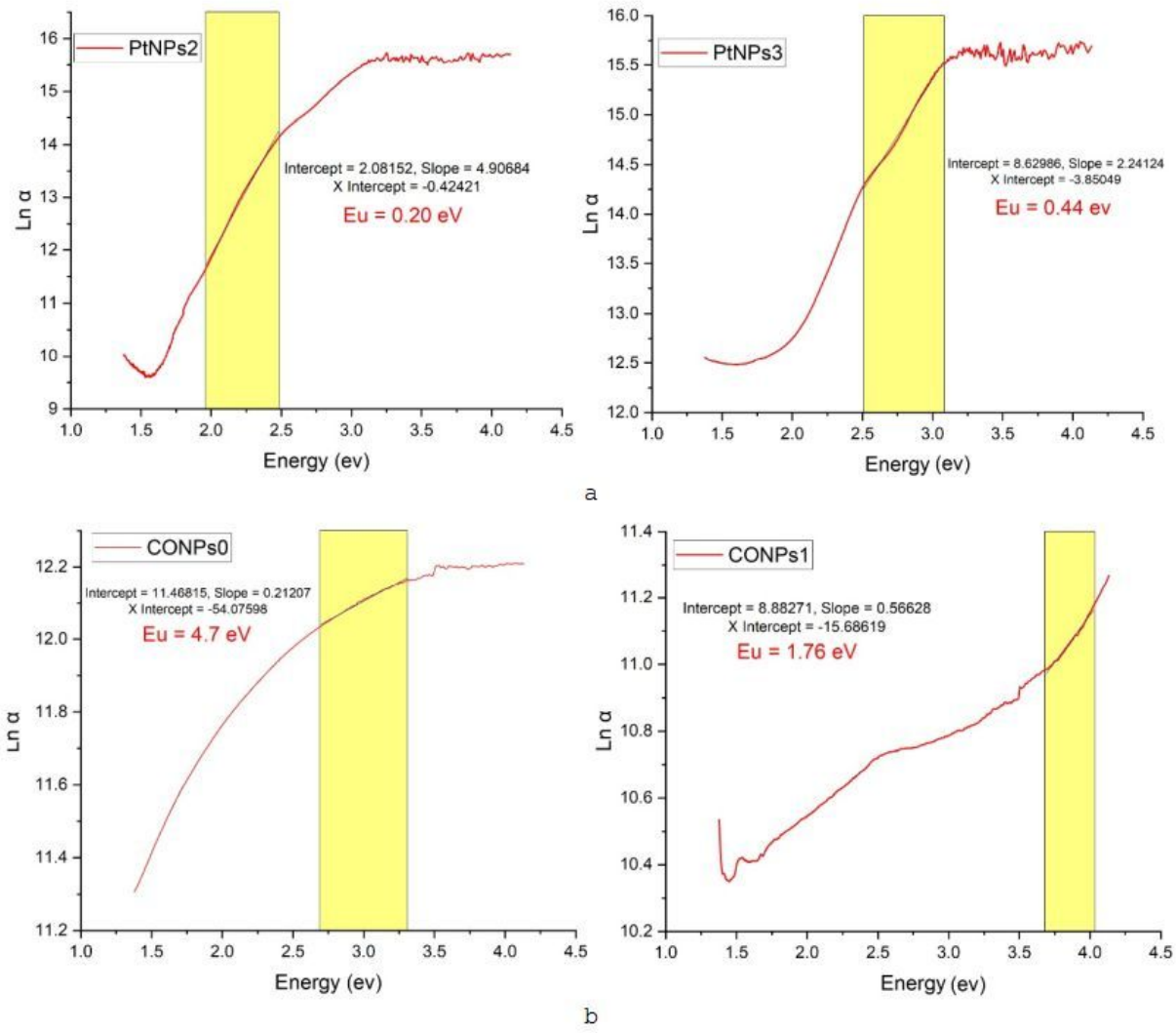

Figure 6

The *lna-hn* graphs of CoNPs and PtNPs obtained under different ablation liquids a) PtNPs and b) CoNPs

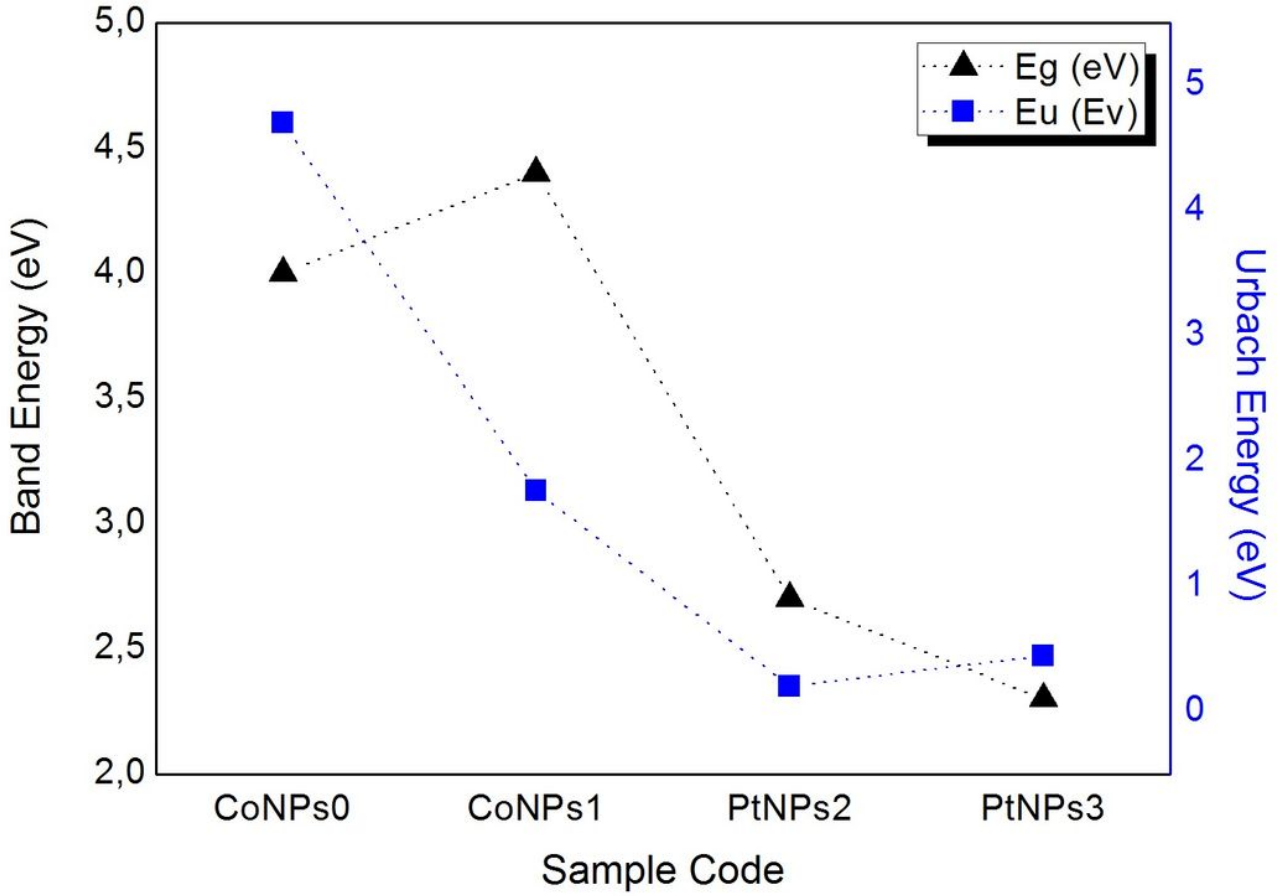

Figure 7

Variation of optical band gap with Urbach energy of CoNPs and PtNPs obtained under different ablation liquids

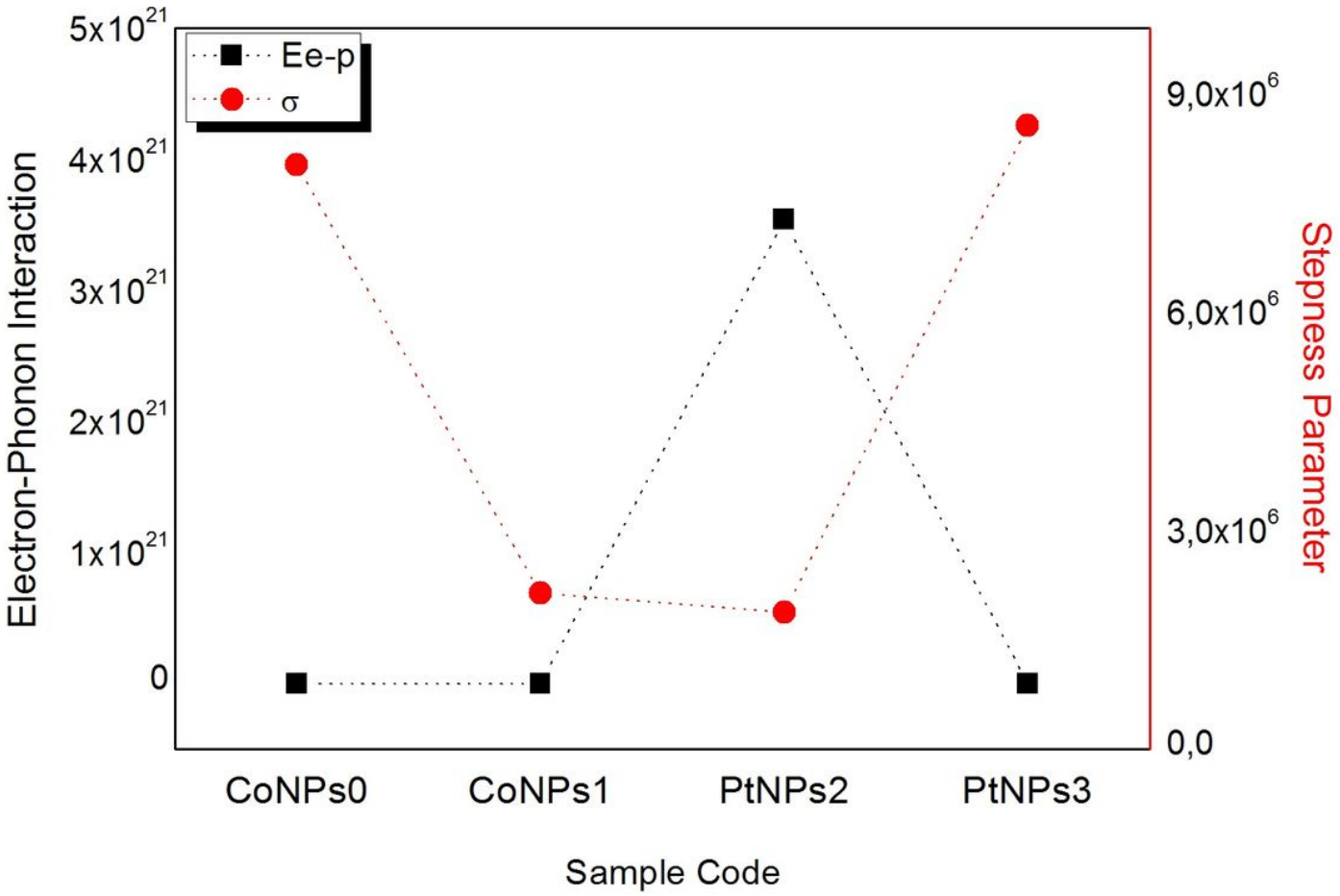

Figure 8

Variation of stepness parameter with electron-phonon intrection of of CoNPs and PtNPs obtained under different ablation liquids

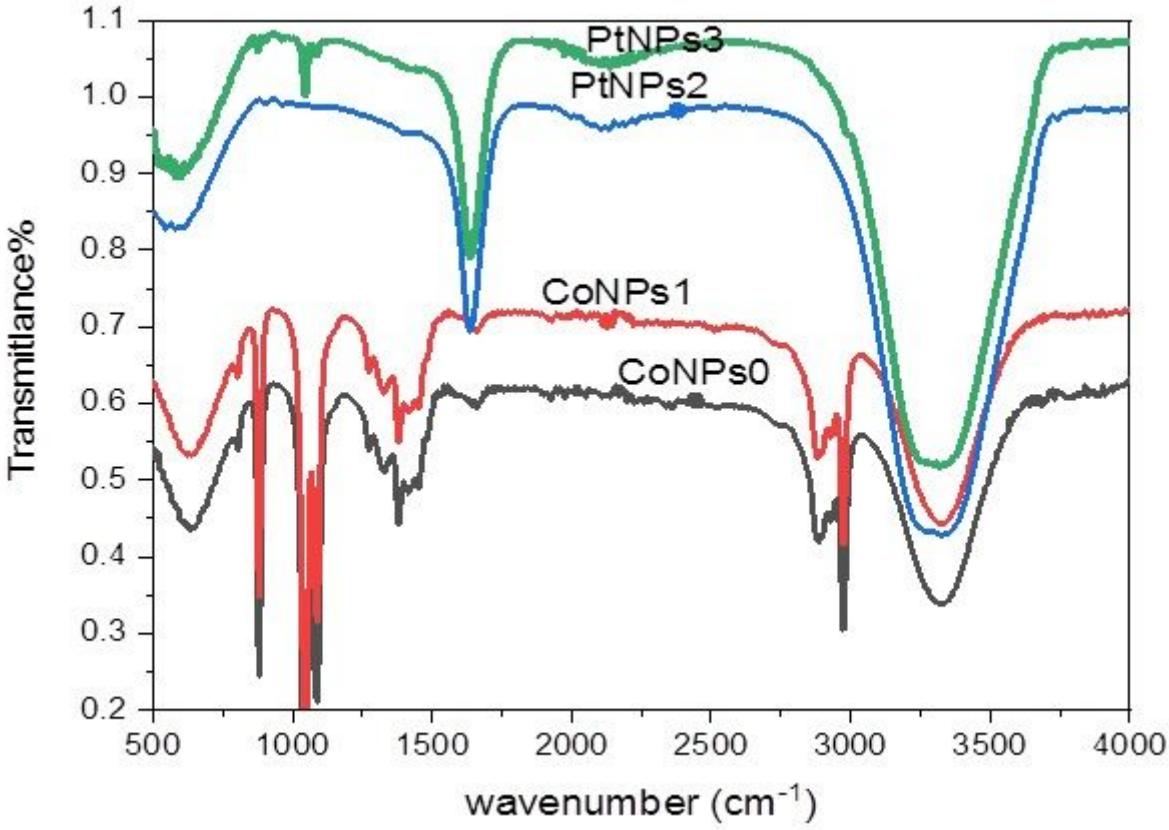

Figure 9

Transmittance spectra of PtNPs and CoNPs nanoparticles obtained under different ablation liquids.

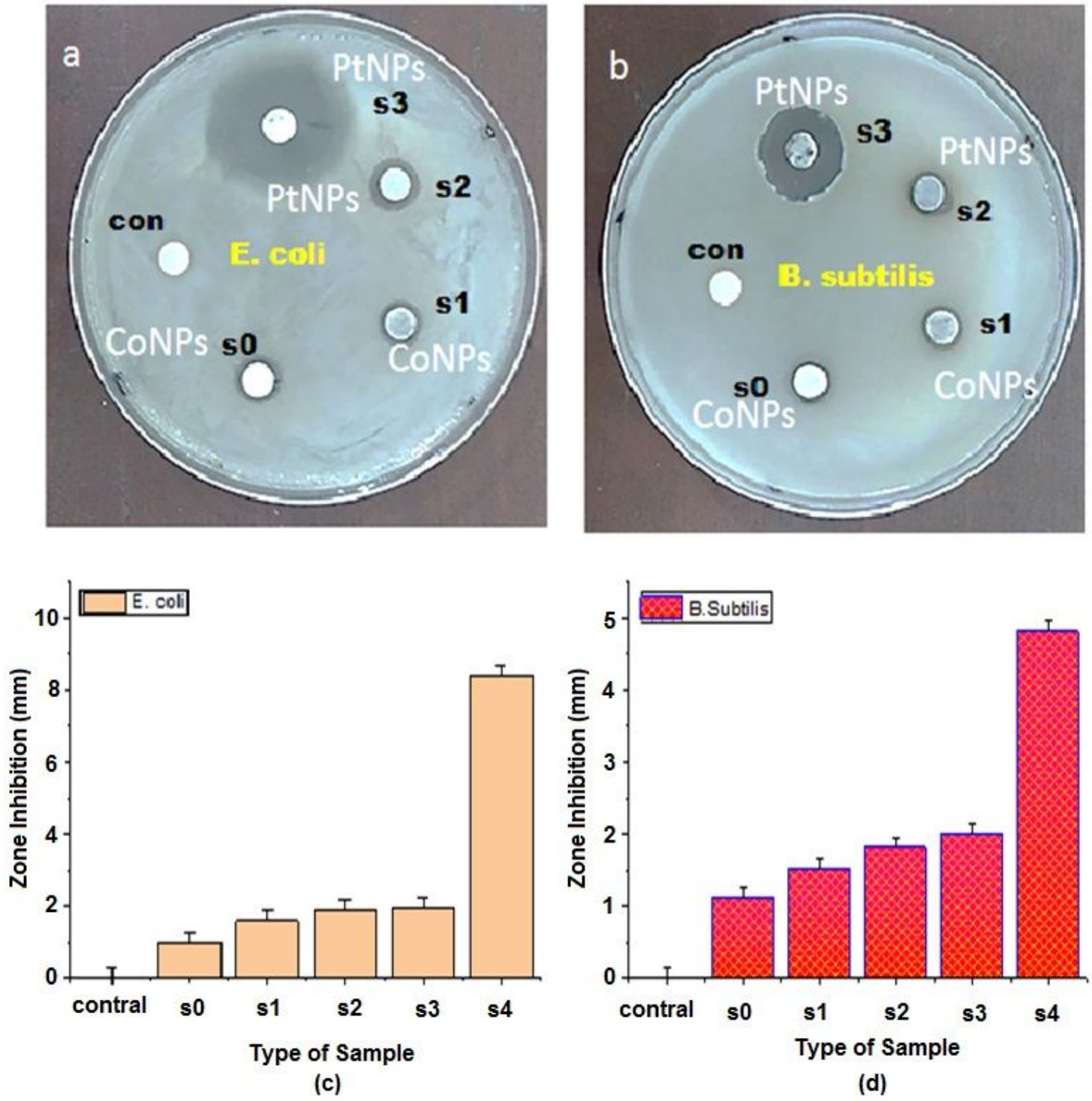

Figure 10

Antibacterial effect of PtNPs and CoNPs nanoparticles obtained under different ablation liquids on two different types of bacteria (a) Zone of inhibition measurements against E. coli (b) Zone of inhibition measurements against B.subtilis) c) Zone inhibition against E. coli and d) Zone inhibition against B. subtilis

Supplementary Files

This is a list of supplementary files associated with this preprint. Click to download.

- GraphicalAbstract.pptx.docx